Figure 1. Locations of the northeast Pacific conductivity−temperature−depth (CTD) stations used in this study superimposed on local bathymetry contours (0, 200, 500, 1000−4000 m levels). These include World Ocean Circulation Experiment (WOCE) stations from the P17C and P17N lines, Multitracers (MT) sites at ~42ºN, and GEOSECS station 201 (GEO−201).

Figure 2. Depth Profiles of $\delta^{13}C_{DIC}$, $[NO_3^-]$ and $[PO_4^{3-}]$ from the four Multitracers sites across the California Current: $\delta^{13}C_{DIC}$, $[NO_3^-]$, and $[PO_4^{3-}]$. Open triangles, MT− INSH (20 km offshore); open squares, MT−NEAR (121 km offshore); open diamonds, MT−MIDW (289 km offshore); and open circles, MT−GYRE (650 km offshore).

Figure 3. The surface $[PO_4^{3-}]$ enrichment across the Multitracers transect. Concentrations of $[NO_3^-]$ are stripped to near zero within the mixed layer which increases in depth from 20 m near the coast to 70 m offshore. Nutrient concentrations below the surface $[PO_4^{3-}]$ enrichment layer follow Redfield scaling relationships. Nutrient axes are scaled by the Redfield $\Delta P/\Delta N$ ratio of 1/16 to demonstrate this relationship.

Figure 4. The correlation of $\delta^{13}C_{DIC}$ and nutrients across the California Current at 42ºN. The relationship of $\delta^{13}C_{DIC}$ versus $[NO_3^-]$ from 0−200 m follows a slope of −0.06 (solid line; r^2 = 0.96), while the relationship for >200 m exhibits a slope of −0.02 (dashed line; r^2 = 0.45). The relationship of $\delta^{13}C_{DIC}$ versus $[PO_4^{3-}]$ from 0−200 m follows a slope of −0.96 (solid line; r^2 = 0.80) while the relationship for >200 m exhibits a slope of −0.30 (dashed line; r^2 = 0.45).

Figure 5. Measurements of $\delta^{13}C_{DIC}$ versus $[NO_3^-]$ in the northeast Pacific. The solid line represents the least squares fit to the 0−200 m data. The anthropogenic $\delta^{13}C_{DIC}$ shift, $\Delta\delta^{13}C_{a-p}$, can be estimated from the offset between the measured $\delta^{13}C_{DIC}$ values and the preanthropogenic model (shaded region). The offset between the preanthropogenic model (shaded region) and the mean ocean biological trend (dashed line) of *Broecker and Maier−Reimer* [1992] gives the size of the local thermodynamic air−sea gas exchange imprint on $\delta^{13}C_{DIC}$. Symbols are the following: open circles, 0−200 m data; open squares, 200−1000 m; filled triangles, 1000−2500 m. (See section 4.2 and 4.3 for details of the preanthropogenic model.)

Figure 6. N* on isopycnal surfaces in the northeast Pacific using WOCE P17 $[NO_3^-]$ and $[PO_4^{3-}]$ measurements. The parameter $N^* = 0.87([NO_3^-]-16[PO_4^{3-}]+2.90)$, as defined by *Gruber and Sarmiento* [1997], provides a quasi−conservative tracer that identifies excesses (positive values) or deficients (negative values) of nitrate relative to phosphate. Scaling for the N* axes is based on the global range of observed values. Dashed vertical line denotes the value of N* where $[NO_3^-]$ and $[PO_4^{3-}]$ = 0. Water mass boundaries are indicated schematically at right.

Figure 7. The anthropogenic $\delta^{13}C_{DIC}$ (filled squares) signature on potential density surfaces (σ_θ) in the northeast Pacific. Vertical lines denote the preanthropogenic constraint of 0‰ (dashed line) and the mixed layer anthropogenic offset, −0.62‰ (solid line). For comparison the mixed layer thermodynamic air−sea gas exchange $\delta^{13}C_{DIC}$ signal is −0.48‰. Water mass boundaries are indicated as in Figure 6.

Figure 8. The distribution of $\Delta^{14}C_{bomb}$ on isopycnal surfaces in the northeast Pacific during 1973 and 1991. The 1973 data are from GEOSECS Station 201 (filled black circles), the 1991 data are from the WOCE P17C (filled dark gray circles), and P17N stations (filled light gray circles) are displayed in Figure 1. The $\Delta^{14}C_{bomb}$ values were estimated using the silica analog method of *Broecker et al*. [1995] with precision of ±10‰. Water mass boundaries indicated as in Figure 6.

Table 1. Estimates of the Global Oceanic Anthropogenic CO_2 Uptake Rate

Source	Approach	Global Uptake Rate, Gt C yr^{-1}
Tans et al. [1993]	air-sea $\delta^{13}C_{DIC}$ disequilibrium	0.6 ± 1.6
Francey et al. [1995]	modification of method of *Tans et al.* [1993]	1.1 ± 1.5[a]
Bacastow et al. [1996]	modeling of mixed layer $\delta^{13}C_{DIC}$ time series	1-4
Quay et al. [1992]	time course change in $\delta^{13}C_{DIC}$ pro files	2.3 ± 1.2
Heimann and Maier-Reimer [1996]	optimization of carbonate chemistry parameterization by "total inversion"	2.1 ± 0.9
Heimann and Maier-Reimer [1996]	"dynamical $^{13}CO_2$ versus CO_2 Constraint"	3.1 ± 1.6

[a] Temporal average and standard deviation derived from 1982 to 1992 annual average estimates.

Table 2. Model Estimates of the Global Oceanic Anthropogenic CO_2 Inventory

Source	Global Uptake Rate, Gt C yr^{-1}	Global Inventory, Gt C	Global Inventory Adjusted to 1991, Gt C
Sarmiento et al. [1995]	1.86	106 in 1982	123
Stocker et al. [1994]	1.99	113 in 1982	131
Sarmiento et al. [1992] as reported by *Sundquist* [1993]	n/a	118 in 1990	120 ± 0.8[a]
Keeling et al. [1989] as reported by *Sundquist* [1993]	n/a	155 in 1990	157 ± 0.8[a]

[a] Adjusted to inferred 1991 levels using the IPCC global uptake rate [*Watson et al.*, 1992] as revised by *Sarmiento and Sundquist* [1992] (i.e., 2.0 ± 0.8 Gt C yr^{-1}).

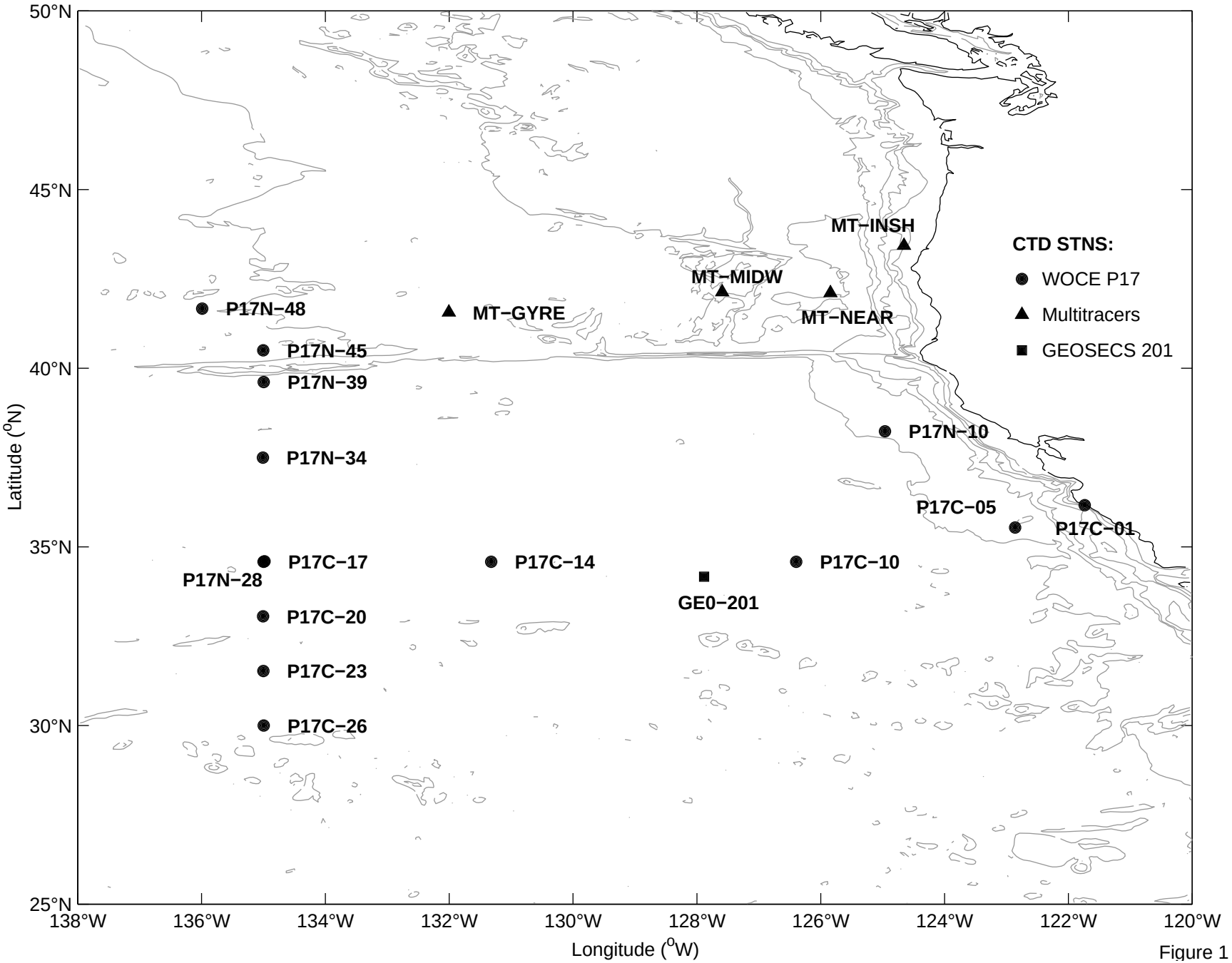
50°N
45°N
40°N
35°N
30°N
25°N
138°W
136°W
134°W
132°W
130°W
128°W
126°W
124°W
122°W
120°W
Latitude (°N)
Longitude (°W)
CTD STNS:
WOCE P17
Multitracers
GEOSECS 201
MT−INSH
MT−MIDW
MT−NEAR
MT−GYRE
P17N−48
P17N−45
P17N−39
P17N−34
P17N−28
P17N−10
P17C−05
P17C−01
P17C−17
P17C−14
P17C−10
GE0−201
P17C−20
P17C−23
P17C−26

Figure 1

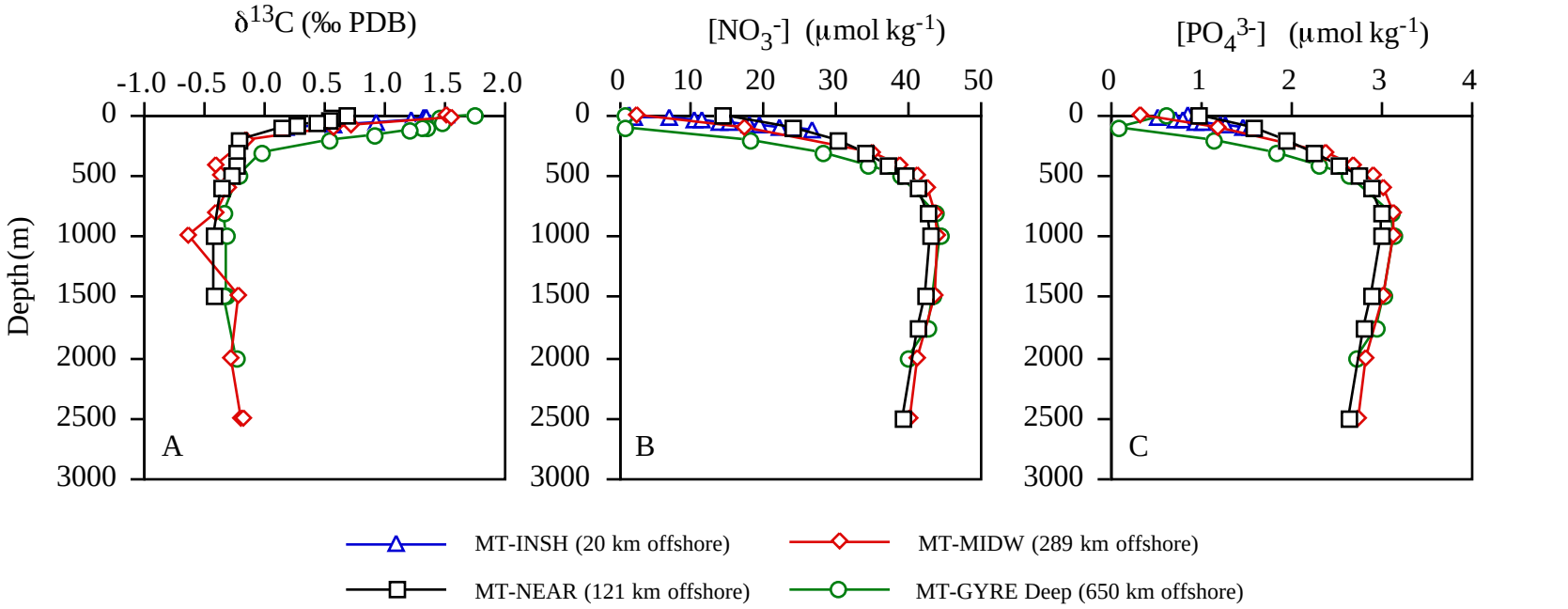
δ13C (‰ PDB)
[NO3-] (µmol kg-1)
[PO43-] (µmol kg-1)
Depth (m)
A
B
C
MT-INSH (20 km offshore)
MT-MIDW (289 km offshore)
MT-NEAR (121 km offshore)
MT-GYRE Deep (650 km offshore)

Top

Figure 2

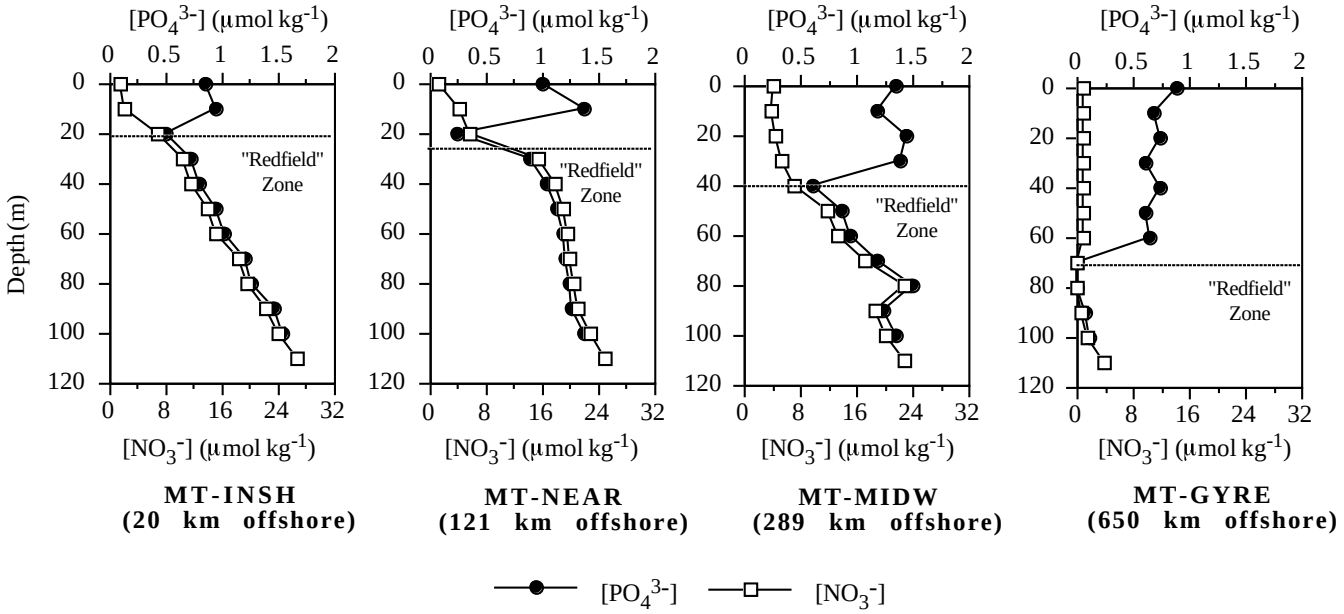
[PO4 3-] (µmol kg-1)
0 0.5 1 1.5 2
0 20 40 60 80 100 120
Depth (m)
"Redfield" Zone
0 8 16 24 32
[NO3-] (µmol kg-1)
MT-INSH (20 km offshore)
MT-NEAR (121 km offshore)
MT-MIDW (289 km offshore)
MT-GYRE (650 km offshore)
[PO4 3-]
[NO3-]

Top

Figure 3

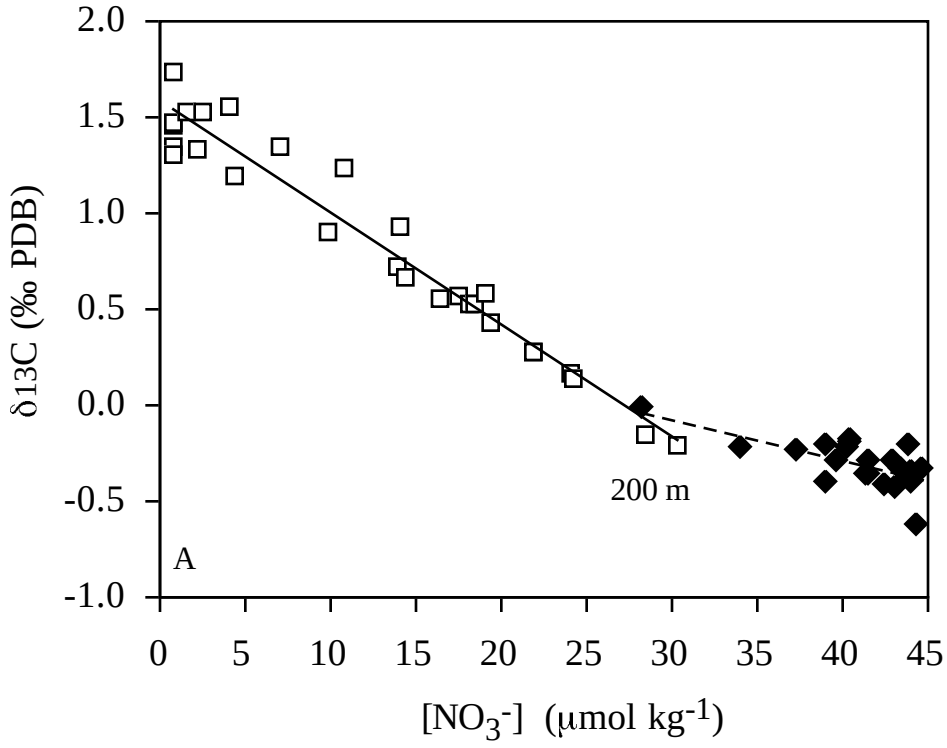
2.0
1.5
1.0
0.5
0.0
-0.5
-1.0
δ13C (‰ PDB)
200 m
A
0
5
10
15
20
25
30
35
40
45
[NO3-] (μmol kg-1)

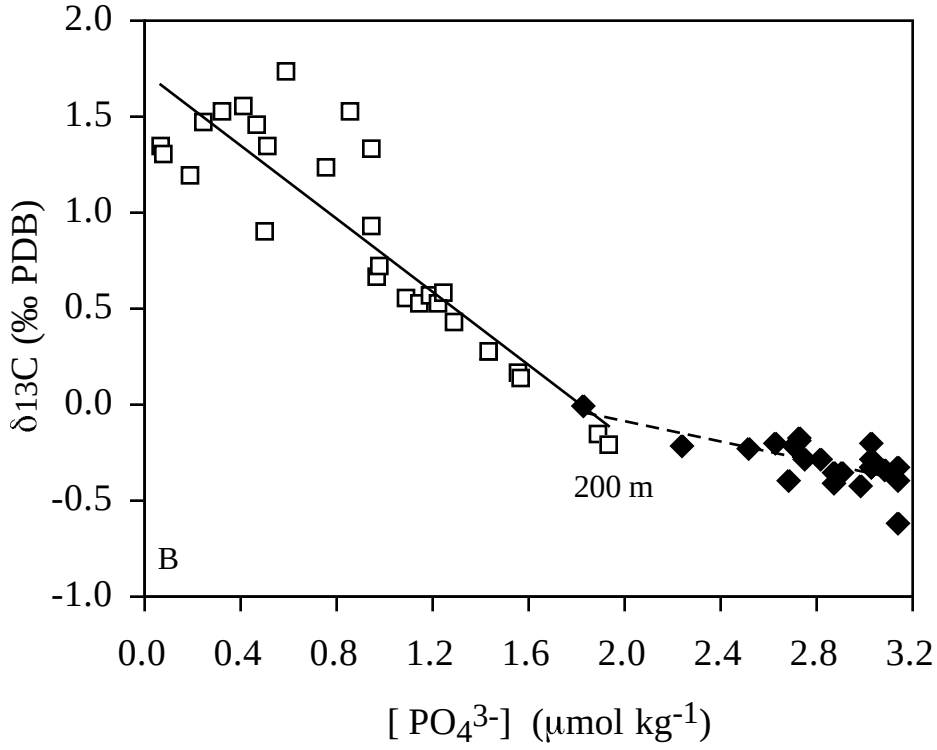
2.0
1.5
1.0
0.5
0.0
-0.5
-1.0
δ13C (‰ PDB)
200 m
B
0.0
0.4
0.8
1.2
1.6
2.0
2.4
2.8
3.2
[PO43-] (μmol kg-1)

Top

Figure 4

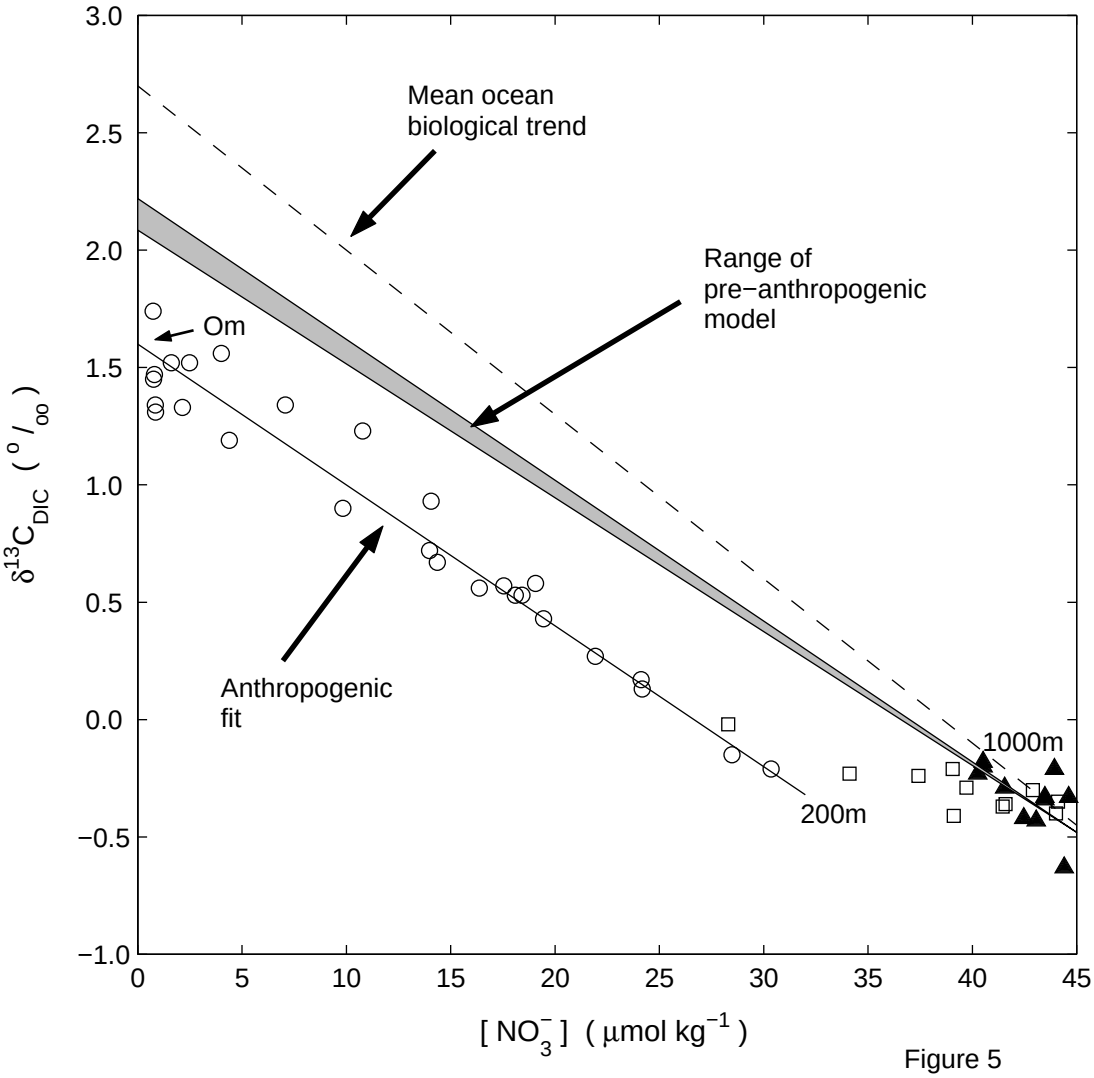
Mean ocean
biological trend
Range of
pre−anthropogenic
model
Om
Anthropogenic
fit
1000m
200m
3.0
2.5
2.0
1.5
1.0
0.5
0.0
−0.5
−1.0
0
5
10
15
20
25
30
35
40
45
δ13CDIC (o/oo)
[NO3−] (µmol kg−1)

Figure 5

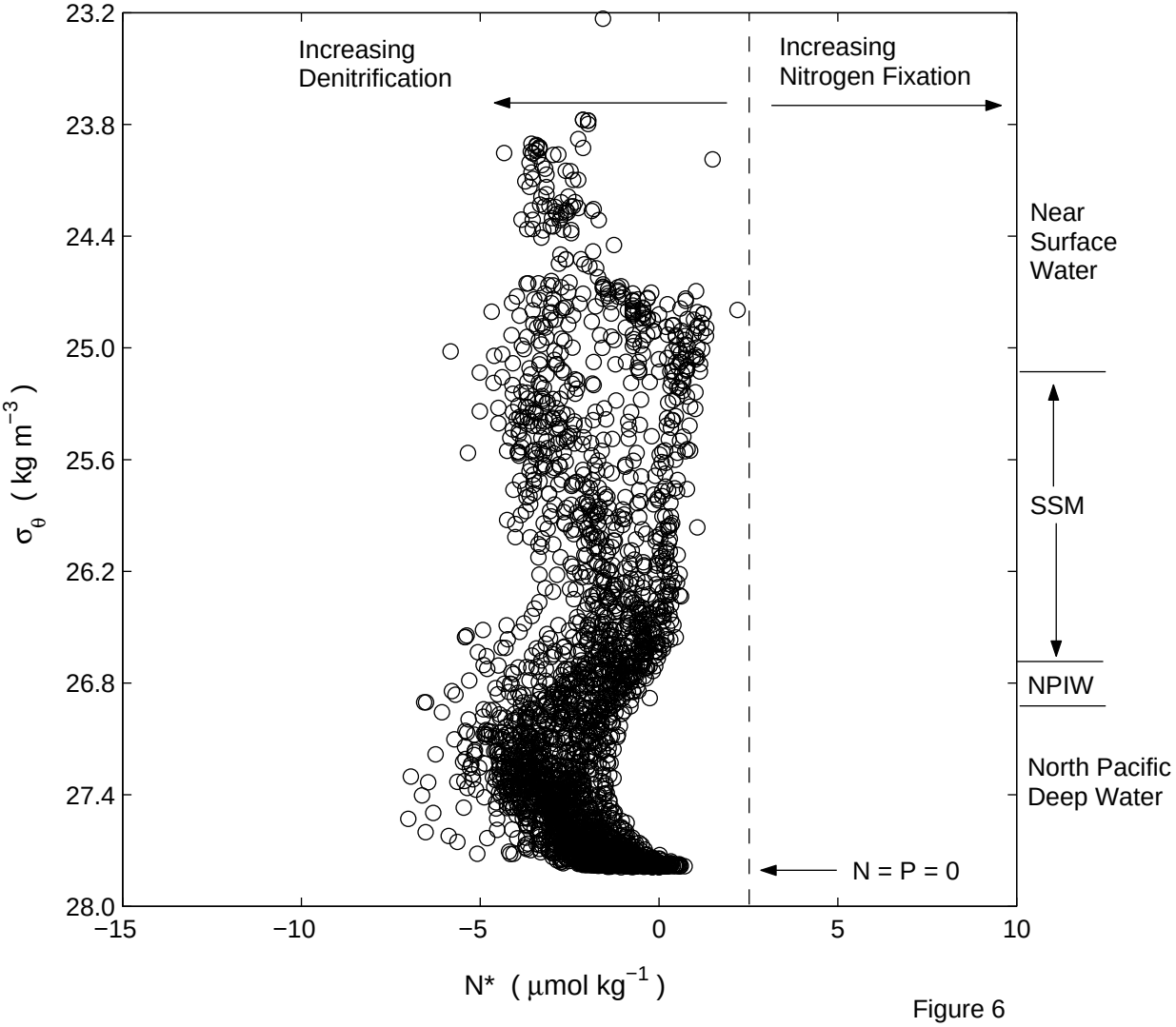
Increasing
Denitrification
Increasing
Nitrogen Fixation
Near
Surface
Water
SSM
NPIW
North Pacific
Deep Water
N = P = 0
23.2
23.8
24.4
25.0
25.6
26.2
26.8
27.4
28.0
−15
−10
−5
0
5
10
σθ (kg m−3)
N* (μmol kg−1)

Figure 6

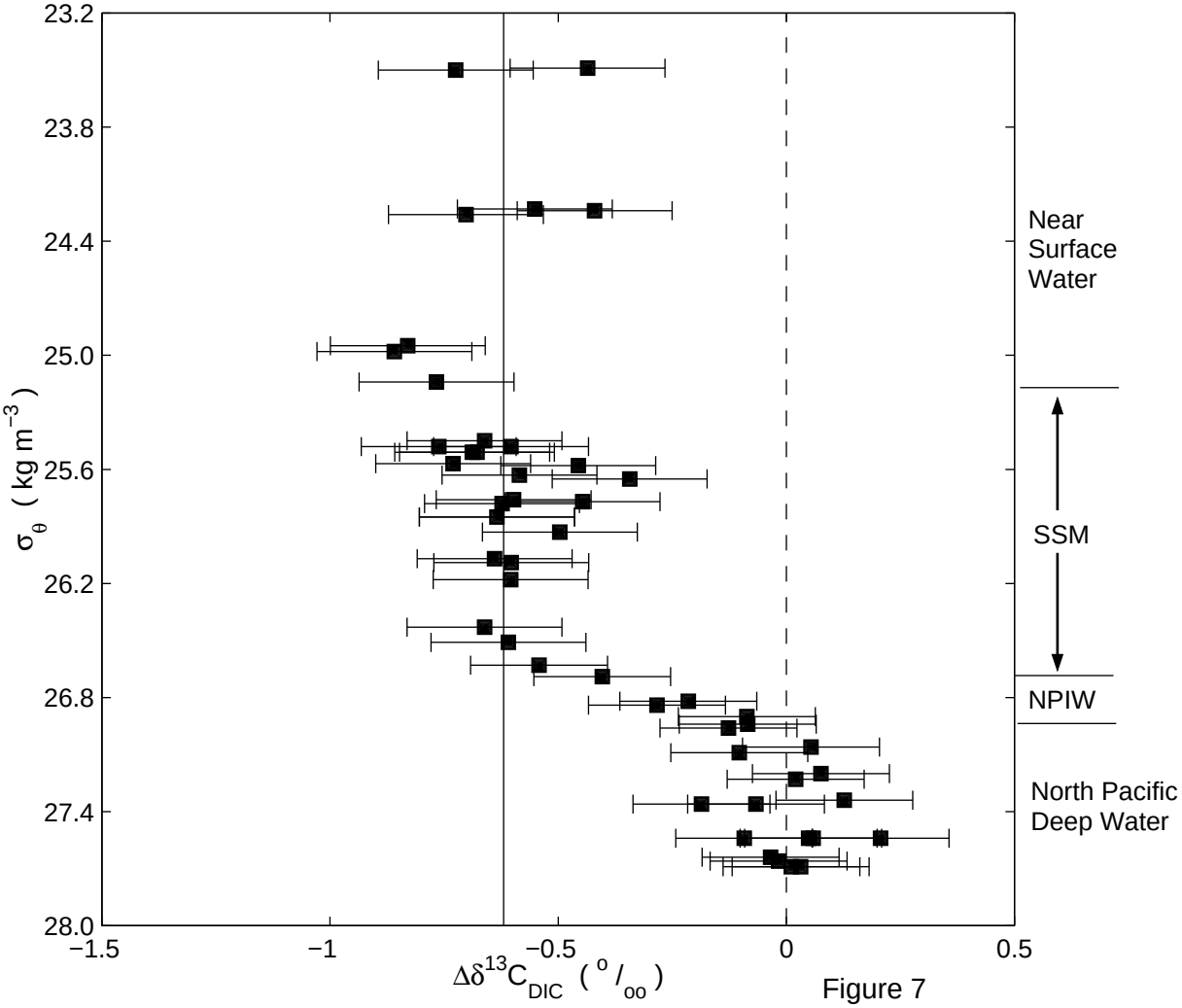
23.2
23.8
24.4
25.0
25.6
26.2
26.8
27.4
28.0
σθ (kg m−3)
−1.5
−1
−0.5
0
0.5
Δδ13CDIC (o /oo)
Near
Surface
Water
SSM
NPIW
North Pacific
Deep Water

Figure 7

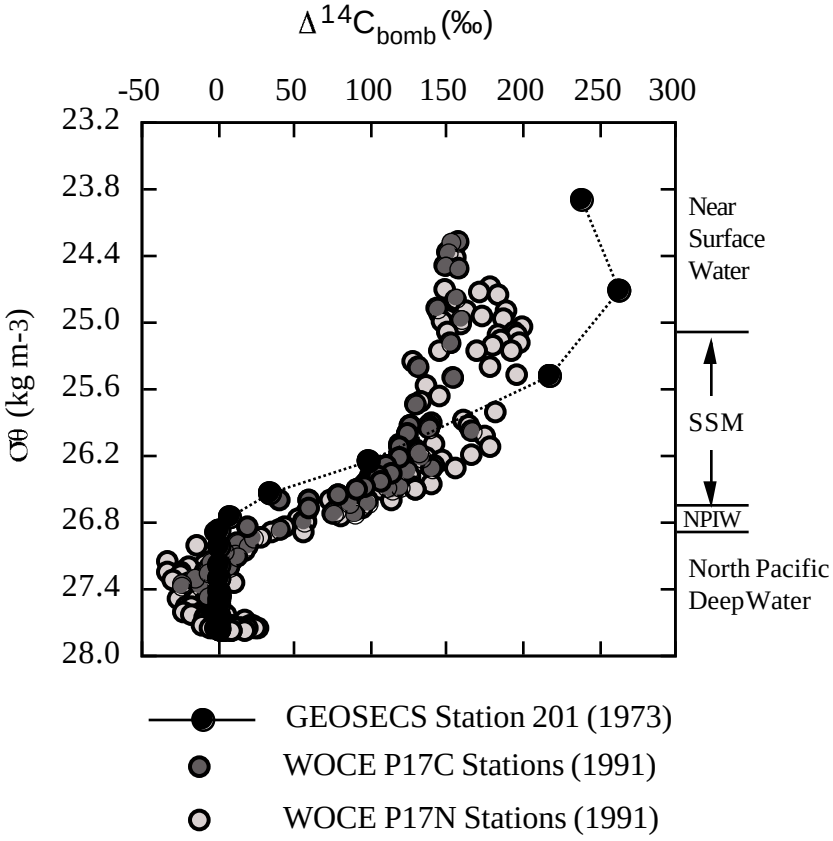
$\Delta^{14}C_{bomb}$ (‰)
-50
0
50
100
150
200
250
300
23.2
23.8
24.4
25.0
25.6
26.2
26.8
27.4
28.0
Oθ (kg m-3)
Near
Surface
Water
SSM
NPIW
North Pacific
Deep Water
GEOSECS Station 201 (1973)
WOCE P17C Stations (1991)
WOCE P17N Stations (1991)

Figure 8